

ActivePose: Active 6D Object Pose Estimation and Tracking for Robotic Manipulation

Sheng Liu^{1,5}, Zhe Li², Weiheng Wang¹, Han Sun^{*2},
Heng Zhang³, Hongpeng Chen⁴, Yusen Qin⁵, Arash Ajoudani³, Yizhao Wang^{†2}

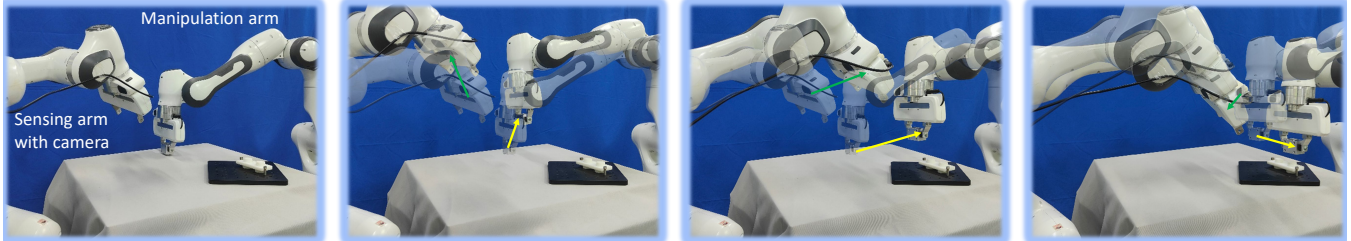


Fig. 1: **ActivePose** integrates an active pose estimation module — resolving pose ambiguities through geometry-aware VLM prompting and NBV planning — with an equivariant diffusion-based active pose tracking module that continuously generates camera trajectories for robotic manipulation.

Abstract— Accurate 6-DoF object pose estimation and tracking are critical for reliable robotic manipulation. However, zero-shot methods often fail under viewpoint-induced ambiguities and fixed-camera setups struggle when objects move or become self-occluded. To address these challenges, we propose an active pose estimation pipeline that combines a Vision-Language Model (VLM) with “robotic imagination” to dynamically detect and resolve ambiguities in real time. In an offline stage, we render a dense set of views of the CAD model, compute the FoundationPose entropy for each view, and construct a geometric-aware prompt that includes low-entropy (unambiguous) and high-entropy (ambiguous) examples. At runtime, the system: (1) queries the VLM on the live image for an ambiguity score; (2) if ambiguity is detected, imagines a discrete set of candidate camera poses by rendering virtual views, scores each based on a weighted combination of VLM ambiguity probability and FoundationPose entropy, and then moves the camera to the Next-Best-View (NBV) to obtain a disambiguated pose estimation. Furthermore, since moving objects may leave the camera’s field of view, we introduce an active pose tracking module: a diffusion-policy trained via imitation learning, which generates camera trajectories that preserve object visibility and minimize pose ambiguity. Experiments in simulation and real-world show that our approach significantly outperforms classical baselines.

I. INTRODUCTION

6D object pose estimation, which recovers an object’s translation and rotation relative to the camera, plays a pivotal role in robotic manipulation tasks such as grasping [1], [2], [3] and assembly [4]. Previous works [5], [6], [7], [8], [9], [10] achieved strong performance by training on specific datasets. More recently, zero-shot methods [11], [12], [13]

demonstrated the ability to estimate poses for novel objects using only their CAD models, without requiring additional real-world annotations.

Despite their strong performance, most existing methods assume that the observation from a single viewpoint contains enough cues to estimate a unique pose. In practice, however, self-occlusion and inter-object occlusion frequently obscure distinctive regions, resulting in fundamentally ill-posed estimation problems. This challenge is especially prevalent in industrial metal parts, where symmetric structures and textureless surfaces inherently reduce distinctive regions, leading to severely exacerbated pose ambiguity.

Since pose ambiguity is inevitable in practical scenarios, resolving it becomes critically important. While physically reorienting the target object or removing occluders can resolve pose ambiguity, such direct interventions are often prohibited in tasks involving high-precision components or delicate instruments. Instead, enabling cameras to actively adjust viewpoints, which mimics human observation, offers a more versatile solution. Although prior studies [14], [15] attempted to predict pose ambiguity, they not only depend on costly prior information, but also fail to provide actionable solutions for ambiguity elimination. Several methods have trained neural networks to predict the Next-Best-View (NBV) for active pose estimation [16], [17], [18]. Although these approaches show promise, they require extensive offline training. Thus, determining optimal camera movements to mitigate pose ambiguity during operation remains an open and challenging problem.

With the above motivation, we propose a geometry-aware prompting framework that integrates a Vision-Language Model (VLM) for zero-shot active 6D pose estimation. In the object geometry understanding stage, a CAD model is used to render a diverse set of viewpoints, and FoundationPose

* Han Sun is the project leader.

† Yizhao Wang is the corresponding author.

Authors Affiliation: ¹Karlsruhe Institute of Technology, Germany, ²Shanghai Jiao Tong University, China, ³Istituto Italiano di Tecnologia, Italy, ⁴The Hong Kong Polytechnic University, Hong Kong, ⁵D-Robotics, China.

[12] produces initial pose estimates; views yielding high pose ambiguity are automatically identified. We then construct an image-based prompt by combining canonical projections (axonometric, bottom, and rear views) with the selected ambiguous view, thereby encoding rich object geometry into the VLM. During online operation, we introduce a VLM-based ambiguity prediction mechanism that determines whether the current camera pose permits a unique estimate. FoundationPose provides candidate poses, from which we compute a pose entropy metric to quantify ambiguity. If the entropy exceeds a threshold, a robot imagination module synthesizes hypothetical views from alternative camera poses; the VLM evaluates these prompts to select the next unambiguous viewpoint, and pose entropy is recomputed to confirm disambiguation. Moreover, when objects are in motion, they may temporarily move out of the camera’s field of view, making it difficult to maintain accurate pose estimates. To handle this, we introduce an active pose tracking module based on an equivariant diffusion policy trained via imitation learning. This module enables the robot to generate smooth camera trajectories that continuously preserve visibility of critical object features and reduce pose ambiguity throughout dynamic manipulation.

To the best of our knowledge, this is the first active pose framework that jointly evaluates pose ambiguity and autonomously adjusts camera viewpoints to actively resolve it. For the benefit of the research community, we will release our code as open source.

In summary, our contributions are:

- We propose a geometry-aware prompting framework that leverages a VLM and per-view pose entropy to enable robust zero-shot ambiguity detection and active 6D pose estimation.
- We introduce a unified scoring mechanism and a differentiable rendering module that selects NBV to resolve ambiguities and improve estimation confidence.
- We present an active pose tracking module based on an equivariant diffusion policy trained via imitation learning, to generate smooth camera trajectories that maintain visibility and accuracy under object motion.
- We validate our framework through extensive experiments in both simulation and the real world, showing improvements over baseline methods.

II. RELATED WORK

A. 6D Pose Estimation

In recent years, 6D pose estimation methods based on single RGBD image using neural networks [5], [6], [7], [19], [20], [21] have outperformed the classic approaches [22]. However, these methods did not consider the ambiguous pose in a specific viewpoint. To address this, active pose estimation techniques adjust the camera viewpoint to improve overall confidence—but they typically rely on object-specific training, hand-crafted heuristics, or expensive annotations [16], [17], [18]. Differently, our approach proactively detects and resolves geometric ambiguities through a zero-shot, geometry-aware framework, employing a differentiable

rendering module that simulates alternative viewpoints for active disambiguation.

B. Vision-Language Models for Robotics

The rapid development of VLMs has further advanced the field of robotics, enabling intelligent agents to interpret natural language commands and reason about visual scenes in a generalizable, task-independent manner [23]. A key advantage of these basic models is that they have been pre-trained on large-scale datasets and can usually be directly deployed in robot systems as high-level planners [24], [25], [26], [27] or low-level controllers [28], [29], [30], [31] without having to learn from scratch, which significantly reduces training costs and improves generalization capabilities. In our work, we use VLMs beyond semantic reasoning—they are also used for geometric disambiguation to support zero-shot active pose estimation.

C. Equivariant Diffusion Models for Robotics

Diffusion-based approaches have recently emerged as a powerful paradigm for robotic manipulation [32]. In particular, equivariant diffusion models exploit the inherent symmetries—such as rotational invariance—present in three-dimensional Euclidean space where robots operate. Existing equivariant diffusion methods can be broadly categorized into two classes: those that predict individual end-effector poses [33], [34], [35], [36], [37] and those that generate complete manipulation trajectories [38], [39], [40], [41]. Building on this, our work introduces a camera tracker based on an equivariant diffusion strategy to minimize pose ambiguity and maintain object visibility during motion.

III. PROBLEM FORMULATION

We formulate active 6D object pose estimation and tracking as a unified decision-making problem. Given only a CAD model of a novel object and an initial camera pose, the goal is to continuously estimate an accurate and unambiguous 6D pose during manipulation. The process begins with zero-shot ambiguity detection: using a geometry-aware prompt and FoundationPose, we query a VLM to compute the pose entropy of the current view. If the entropy exceeds a threshold, indicating high ambiguity, we select a NBV from a predefined candidate set. This is done via differentiable view synthesis, where virtual viewpoints are rendered, scored by the VLM and pose entropy, and ranked to identify the most informative view. In parallel, under continuous object motion and occlusion, learn an active tracking policy by training an equivariant diffusion model on demonstration data so that the robot can generate camera trajectories that keep the object in view, thereby ensuring high-precision manipulation.

IV. METHOD

Our approach comprises two tightly integrated modules: an active pose estimation pipeline that resolves 6-DoF pose ambiguities (Algorithm 1), and an active pose tracking module that maintains accurate pose estimation during object motion using an equivariant diffusion policy (Algorithm 2).

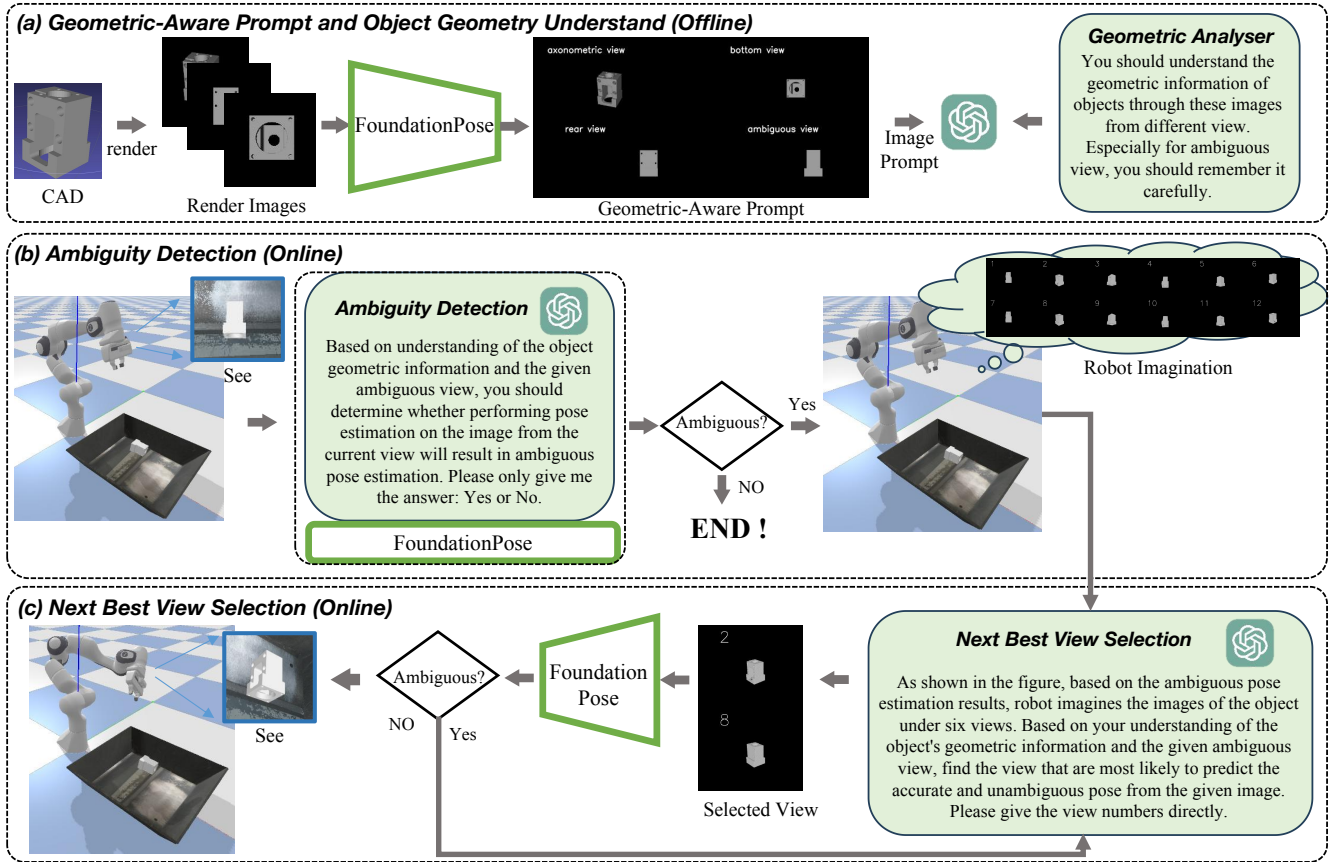


Fig. 2: **Pipeline of Active Pose Estimation.** (1) Offline: The system computes pose entropy from rendered views and constructs a geometry-aware prompt using ambiguous and unambiguous examples. (2) Online: It assesses ambiguity from the live image via a VLM and selects the NBV through rendering and entropy-guided scoring.

A. Active Pose Estimation

Our active pose estimation pipeline (see Fig. 2) comprises two tightly-coupled stages: *offline geometric-aware prompt construction* and *online ambiguity detection with next-best-view selection*. Given a live image I_{live} and its camera-to-base transform T_b^c , we proceed as follows.

We first render a dense set of views $\{R_k\}$ of the CAD model. For each rendered view R_k , we invoke FoundationPose to obtain its 6-DoF rotation distribution and compute its Shannon entropy $H_k = \text{Entropy}(\text{FoundationPose}(R_k))$. We then sort the views by H_k and select a set U of the lowest-entropy “unambiguous” views (e.g., axonomic, bottom, rear) and a set A of the highest-entropy “ambiguous” views. The geometric-aware prompt is constructed by aggregating the images in $U \cup A$. At runtime, we acquire the live image I_{live} and compute the ambiguity probability $p_{\text{amb}} = P_{\text{VLM}}(\text{“ambiguous”} \mid I_{\text{live}}, \text{prompt})$. If $p_{\text{amb}} < \tau$ (with threshold $\tau = 0.5$), we immediately invoke $T_s^c = \text{FoundationPose}(I_{\text{live}})$ to obtain the final 6-DoF pose. Otherwise, for each candidate virtual camera pose C_j we render the imagined view $\hat{I}_j = \text{Render}(C_j)$, compute the secondary ambiguity probability $p_{\text{amb},j} = P_{\text{VLM}}(\text{“ambiguous”} \mid \hat{I}_j, \text{prompt})$, and compute its pose entropy $H_j = \text{Entropy}(\text{FoundationPose}(\hat{I}_j))$. After com-

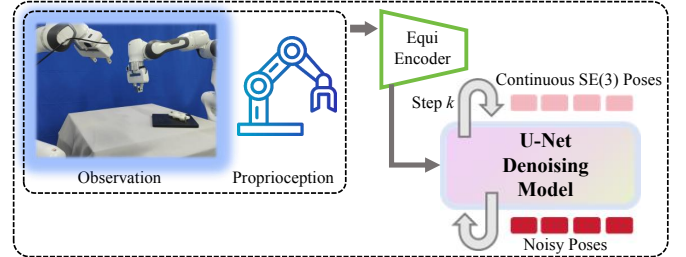


Fig. 3: **Pipeline of Active Pose Tracking.** Encode the current observation, denoise over K reverse-diffusion steps to obtain continuous SE(3) poses, then execute the last k poses in a receding-horizon loop.

puting a combined score for each candidate view as $S_j = \lambda H_j + (1 - \lambda)p_{\text{amb},j}$, which balances geometric uncertainty (entropy) and semantic ambiguity, We then select the index $j^* = \arg \min_j S_j$, move the camera to C_{j^*} , capture a new live image I_{live}^* , and invoke $T_s^c = \text{FoundationPose}(I_{\text{live}}^*)$ to obtain the final, disambiguated pose (see Algorithm 1).

B. Active Pose Tracking

After obtaining the object’s 6D pose, we formulate active tracking as a *conditional diffusion* problem to maintain

Algorithm 1 Active Pose Estimation

Require: CAD model, candidate poses $\{C_j\}_{j=1}^M$, threshold τ , fusion weight λ

Ensure: final 6-DoF pose T_s^c

- 1: Render dense views $\{R_k\}$ of the CAD model
- 2: **for all** R_k in $\{R_k\}$ **do**
- 3: $H_k \leftarrow \text{Entropy}(\text{FoundationPose}(R_k))$
- 4: **end for**
- 5: Select unambiguous views U with lowest H_k and ambiguous views A with highest H_k
- 6: $\text{prompt} \leftarrow U \cup A$
- 7: Acquire live image I_{live}
- 8: $p_{\text{amb}} \leftarrow P_{\text{VLM}}(\text{"ambiguous"} \mid I_{\text{live}}, \text{prompt})$
- 9: **if** $p_{\text{amb}} < \tau$ **then**
- 10: $T_s^c \leftarrow \text{FoundationPose}(I_{\text{live}})$
- 11: **else**
- 12: **for** $j = 1, \dots, M$ **do**
- 13: $\hat{I}_j \leftarrow \text{Render}(C_j)$
- 14: $p_{\text{amb},j} \leftarrow P_{\text{VLM}}(\text{"ambiguous"} \mid \hat{I}_j, \text{prompt})$
- 15: $H_j \leftarrow \text{Entropy}(\text{FoundationPose}(\hat{I}_j))$
- 16: $S_j \leftarrow \lambda H_j + (1 - \lambda)p_{\text{amb},j}$
- 17: **end for**
- 18: $j^* \leftarrow \arg \min_j S_j$
- 19: Move camera to C_{j^*} and acquire I_{live}^*
- 20: $T_s^c \leftarrow \text{FoundationPose}(I_{\text{live}}^*)$
- 21: **end if**

continuous visibility and precise pose accuracy (see Fig. 3). Instead of hand-crafting a replanning objective, we train an *equivariant diffusion network* to imitate demonstrated camera motions. At each time step t , we build the observation $O_t = \{ {}^oT_b^{t-H+1:t}, {}^eT_b^{t-H+1:t} \}$, containing the past H frames of (i) the object’s pose in the robot-base frame oT_b and (ii) the end-effector’s pose eT_b .

We initialize a standard Gaussian noise A_t^K , then apply K learned reverse-diffusion steps via

$$A_t^{k-1} = \alpha_k \left(A_t^k - \gamma_k \epsilon_\theta(O_t, A_t^k, k) \right) + \sigma_k \mathcal{N}(0, I), \quad (1)$$

$$\mathcal{L} = \mathbb{E} \left[\left\| \epsilon_k - \epsilon_\theta(O_t, \hat{\alpha}_k A_t^0 + \hat{\beta}_k \epsilon_k, k) \right\|^2 \right], \quad (2)$$

where $\alpha_k, \gamma_k, \sigma_k$ (and their one-step equivalents $\hat{\alpha}_k, \hat{\beta}_k$) define the DDIM noise schedule [42], and rotations use the continuous 6D representation [43]. Our ϵ_θ is a lightweight equivariant convolutional network, and we predict *samples* rather than noise for faster inference.

At runtime, we use a receding-horizon scheme: after denoising to obtain $\{A_t^0\} \equiv \{e\hat{T}_b^{t+1:t+K}\}$, we execute the last k poses, then roll the window forward and repeat. This yields smooth, adaptive camera motions that naturally keep the object in view and maintain pose accuracy—without requiring an explicit entropy-minimization term, as ambiguity reduction emerges implicitly from the learned policy.

V. EXPERIMENTS

In this section we describe our hardware/software setup, implementation details, and evaluation protocol, then report

Algorithm 2 Active Pose Tracking

Require: Object pose in camera frame oT_c , end-effector pose in base frame eT_b , camera pose in end-effector frame eT_c ,

- 1: history length H , prediction horizon K , rollout length k , total steps N .

Ensure: Executed end-effector trajectory $\{{}^eT_b\}_{t=1}^N$

Preprocessing: \triangleright Notation ${}^{\text{ref}}T_{\text{tgt}}$

- 2: Compute camera-to-object transform:

$${}^cT_o \leftarrow ({}^oT_c)^{-1}$$
- 3: Compute base-to-end-effector transform:

$${}^bT_e \leftarrow ({}^eT_b)^{-1}$$
- 4: Compute object pose in base frame:

$${}^bT_o \leftarrow {}^bT_e \cdot {}^eT_c \cdot {}^cT_o$$
- 5: **for** $t = 1$ **to** N **do**
- 6: Collect history: $\{ {}^bT_o^{t-H+1:t} \}, \{ {}^bT_e^{t-H+1:t} \}$
- 7: Sample future end-effector poses:

$$\{ {}^b\hat{T}_e^{t+1:t+K} \} \leftarrow \text{DP}(O_t)$$

\triangleright see Eqs. (1)–(2)
- 8: **Execute last k steps** of the predicted poses:

$$\{ {}^b\hat{T}_e^{t+K-k+1:t+K} \}$$
- 9: Append executed poses to trajectory
- 10: $t \leftarrow t + k$
- 11: **end for**

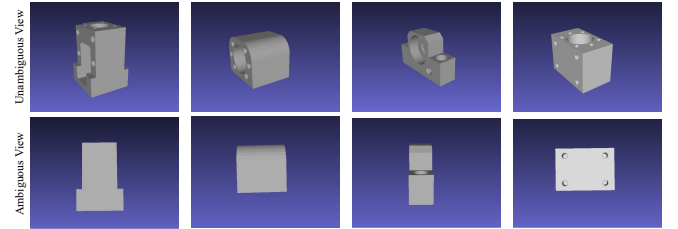


Fig. 4: CAD models of the experimental objects (Obj. 1–3 from MP6D; Obj. 4 for assembly) and an example ambiguous view.

results for both active pose estimation and active pose tracking on challenging manipulation tasks.

A. Experimental Setups

Implementation Details. For **active pose estimation**, we conduct experiments in both simulation and the real world. The simulation experiments are implemented in PyBullet [44], which provides a controlled environment for rendering candidate viewpoints and selecting the NBV. For **active pose tracking** and **Integrated Scenarios**, we exclusively perform real-robot evaluations.. All real-world experiments are performed on two Franka Emika Panda 7-DOF arms: one *sensing arm* carries a wrist-mounted Intel RealSense D435

RGB-D camera (640×480 @ 30Hz) for observation, while the second *manipulation arm* is equipped with a parallel-jaw gripper (see Fig. 1).

As shown in Fig. 4, we select three objects from MP6D [45] for evaluation, and choose another one object for the assembly task. All four selected objects exhibit high pose ambiguity, making them suitable for testing both ambiguity detection and active viewpoint selection.

For the *active pose estimation* pipeline, we call the ChatGPT4o API as our VLM. Each live RGB frame is cropped and resized to 224×224, then paired with a geometry-aware prompt. We render $M = 12$ candidate viewpoints per ambiguous detection, set the fusion weight $\lambda = 0.6$, and use FoundationPose v1.0 to produce 6-DoF estimation and entropy computation.

For the *active pose tracking* module, we collect 10 expert demonstrations per task, each consisting of ~ 200 frames of object and end-effector poses at 10 Hz. We train the equivariant diffusion policy with AdamW (batch size 40, LR 3×10^{-4}) for 2,000 epochs. During inference, the policy predicts $K = 20$ future end-effector actions; we execute the last $k = 5$ before replanning. All training and inference run on a single NVIDIA RTX 4090 GPU.

Estimation Scenarios. We evaluate active pose estimation under two conditions:

- 1) *Random Placement*: each object is placed at a random position and orientation on the workspace.
- 2) *High-Entropy Placement*: each object is deliberately positioned at a precomputed high-entropy (ambiguous) viewpoint.

Estimation Evaluation Baselines.

- **Fixed-View**: run FoundationPose once on the initial camera pose, with no NBV selection.
- **Random-NBV**: upon ambiguity detection, randomly choose one of the M candidate viewpoints for a second FoundationPose estimate.

Estimation Evaluation Metrics. We report the *success rate* (SR), defined as the percentage of trials where the final estimated 6D pose has a translation error below 5mm and a rotation error below $\leq 5^\circ$. Each method is tested in 10 trials per scenario.

Tracking Scenarios. We test all trackers under four challenging conditions:

- 1) *Long-range linear motion*: An object moves from point A to point B along a straight trajectory, where point B is at a random location.
- 2) *Circular rotational motion*: the object rotates around a fixed point on the table.
- 3) *Temporary occlusion*: the object is briefly occluded (up to 1s) during tracking, testing the system’s ability to maintain pose estimation or recover upon reappear-ance.
- 4) *Random spatial motion*: the object undergoes unpredictable translational and rotational movements in 3D

space, including sharp turns and speed variations, stressing the tracker’s ability to stably follow erratic trajectories.

Tracking Baselines. For the *active pose tracking* component, we compare our diffusion-policy tracker to:

- **Pose-Servo**: A classical pose-based visual servoing baseline. The wrist-mounted camera provides the current 6-DoF object pose; a proportional controller converts the pose error into end-effector velocity commands.
- **World-Camera**: A fixed, calibrated overhead camera continuously tracks the object’s 6-DoF pose via FoundationPose.

Tracking Evaluation Metrics. We report the *success rate* (SR) for each trial: the fraction of runs in which the method completes the task without any “pose-loss” event. Each method was evaluated in 20 independent trials in each scenario.

Integrated Estimation & Tracking Scenarios. To validate the combined benefits of active pose estimation and active pose tracking, we evaluate on a standard peg-in-hole assembly task: the robot grasps an object from the tabletop and then inserts it into a fixed socket whose position is randomized before each run. The assembly task itself is not the focus of this paper, so we directly use the assembly policy in [46].

Combined Baselines.

- **Fixed-View**: perform FoundationPose once with a single, fixed world camera view and execute assembly task based on that estimation.
- **Fixed-View + Pose-Servo**: run FoundationPose once on the initial grasp view, then classical Pose-Servo for assembly.
- **Random-NBV + Pose-Servo**: upon detecting ambiguity at grasp, select one random NBV for a second FoundationPose estimate, then Pose-Servo.

Metric. We report *Success Rate* (SR): the fraction of trials that complete peg-in-hole task. Each method is evaluated in 10 trials.

B. Experimental Results

Active Pose Estimation Results. For active pose estimation, we evaluate two placement conditions—Random Placement and High-Entropy Placement (deliberately ambiguous starts). In simulation (Table I), the **Fixed-View** baseline attains only 60.0% SR under Random Placement but drops to 20.0% SR under High-Entropy Placement. **Random-NBV** selection improves SR to 62.5% and 52.5%, respectively. In contrast, our active pose estimation pipeline achieves 97.5% SR on Random Placement and 95.0% SR on High-Entropy Placement, showing strong performance across both scenarios.

In real-world trials (Table II), **Fixed-View** SR is 57.5% (Random) versus 20.0% (High-Entropy), and **Random-NBV** reaches 50.0% in both cases. Our method maintains high SR

TABLE I: Success Rate (SR) of Active Pose Estimation in Two Scenarios (Simulation)

Method	Random Placement					High-Entropy Placement				
	Obj 1	Obj 2	Obj 3	Obj 4	SR	Obj 1	Obj 2	Obj 3	Obj 4	SR
Fixed-View	70.0%	50.0%	50.0%	70.0%	60.0%	40.0%	10.0%	20.0%	10.0%	20.0%
Random-NBV	70.0%	50.0%	70.0%	60.0%	62.5%	60.0%	40.0%	60.0%	50.0%	52.5%
Ours	100.0%	100.0%	100.0%	90.0%	97.5%	100.0%	90.0%	100.0%	90.0%	95.0%

TABLE II: Success Rate (SR) of Active Pose Estimation in Two Scenarios (Real)

Method	Random Placement					High-Entropy Placement				
	Obj 1	Obj 2	Obj 3	Obj 4	SR	Obj 1	Obj 2	Obj 3	Obj 4	SR
Fixed-View	70.0%	50.0%	50.0%	60.0%	57.5%	30.0%	20.0%	20.0%	10.0%	20.0%
Random-NBV	70.0%	60.0%	70.0%	50.0%	62.5%	60.0%	50.0%	60.0%	30.0%	50.0%
Ours	90.0%	90.0%	100.0%	90.0%	92.5%	100.0%	90.0%	100.0%	90.0%	95.0%

TABLE III: Success Rate (SR) of Active Pose Tracking across Four Scenarios

Method	Long-range Linear Motion					Circular Rotational Motion					Temporary Occlusion					Random Spatial Motion				
	Obj 1	Obj 2	Obj 3	Obj 4	SR	Obj 1	Obj 2	Obj 3	Obj 4	SR	Obj 1	Obj 2	Obj 3	Obj 4	SR	Obj 1	Obj 2	Obj 3	Obj 4	SR
Pose-Servo	65.0%	70.0%	60.0%	50.0%	61.3%	0.0%	0.0%	0.0%	0.0%	0.0%	0.0%	0.0%	5.0%	0.0%	1.3%	50.0%	45.0%	50.0%	55.0%	50.0%
World-Camera	50.0%	45.0%	65.0%	35.0%	48.8%	65.0%	60.0%	75.0%	50.0%	62.5%	35.0%	15.0%	15.0%	5.0%	17.5%	70.0%	55.0%	65.0%	45.0%	58.8%
Ours	85.0%	90.0%	80.0%	95.0%	87.5%	80.0%	90.0%	95.0%	100%	91.3%	50.0%	45.0%	65.0%	50.0%	52.5%	70.0%	75.0%	65.0%	80.0%	72.5%

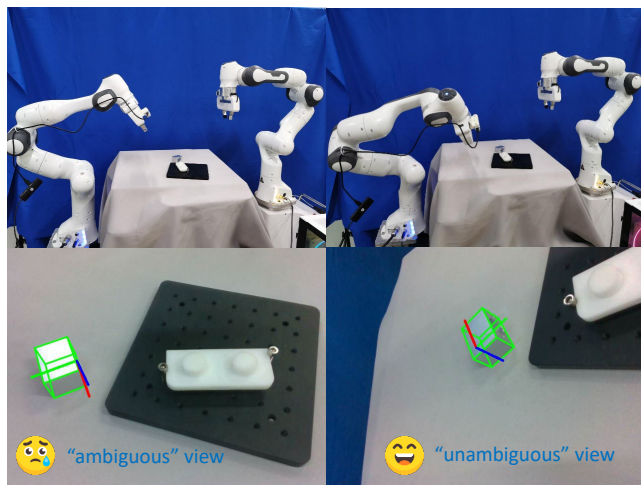


Fig. 5: An example of successful pose estimation.

TABLE IV: Success Rate of Peg-in-Hole Assembly

Method	Success Rate
Fixed-View	40%
Fixed-View + Pose-Servo	50%
Random-NBV + Pose-Servo	70%
Ours	90%

of 92.5% and 95.0%, respectively. Although the success rates are slightly lower than in simulation—likely due to sensor noise and calibration errors—the performance remains consistently high. Figure 5 illustrates an example of successful pose estimation in the real world.

Active Pose Tracking Results. Table III reports the success rate (SR) for each object over 20 trials across four tracking scenarios. In *long-range linear motion*, **Pose-Servo** attains 61.3% SR—the commanded motions can exceed the

robot’s reachable workspace—while **World-Camera** reaches only 48.8% as the object leaves its fixed field of view (FOV). Our diffusion-policy tracker predicts intermediate waypoints and adapts smoothly, yielding 87.5% SR. Under *circular rotation*, **Pose-Servo** invariably fails (0.0%) due to unreachable orientations, and **World-Camera** scores 62.5% when the object rotates beyond its fixed FOV; in contrast, our method maintains 91.3% by continuously adjusting the camera pose. With *temporary occlusions*, **Pose-Servo** and **World-Camera** attain only 1.3% and 17.5% SR, respectively, whereas our tracker achieves 52.5% by reliably reacquiring the object—despite the challenge of rapid occlusions. Under *random spatial motion*, baselines score 50.0% (**Pose-Servo**) and 58.8% (**World-Camera**), compared to 72.5% for our approach, demonstrating superior adaptability to unpredictable trajectories.

Peg-in-Hole Assembly Results. Table IV presents the success rates (SR) for the peg-in-hole task in 10 trials per method. **Fixed-View** achieves 40% SR, as the randomly placed socket can fall outside the fixed camera’s FOV. Adding a **classic Pose-Servo** system under the same fixed view improves the SR to 50%, but the servo control often fails to reach the desired end-effector pose, leading to failures. Introducing a **single Random-NBV** raises the SR to 70% by reducing the initial ambiguity, yet the fixed camera servo system still struggles with unreachable poses.

Our ActivePose framework achieves a 90% SR by selecting disambiguating viewpoints during grasp and employing a diffusion-based policy to continuously track the object into the socket. This ensures persistent visual contact throughout the assembly process—something the fixed World-Camera baseline cannot provide—while also avoiding the strict end-effector pose constraints required by classical Pose-Servo approaches.

VI. CONCLUSION AND FUTURE WORK

In this paper, we present ActivePose, a unified framework for active 6D object pose estimation and tracking. Our approach leverages a geometry-aware prompt with a Vision-Language Model (VLM) for zero-shot ambiguity detection, and combines a differentiable “robot imagination” module with FoundationPose’s entropy metric to select Next-Best-View (NBV) for pose disambiguation. In addition, an equivariant diffusion-policy tracker generates camera trajectories during manipulation, thereby ensuring accurate pose estimation throughout the entire process. ActivePose achieves consistently higher success rates in both simulation and real-world experiments than classical baselines, demonstrating robust pose disambiguation and accurate pose estimation throughout the manipulation process.

However, we observe that although the equivariant diffusion policy produces smooth camera trajectories, our current approach relies heavily on pose as the input feature, making it more sensitive to rotational variations than to translational ones. In future work, we plan to explore more suitable input representations, such as incorporating image-based features.

VII. ACKNOWLEDGMENTS

We used ChatGPT (OpenAI, GPT-5) to aid literature searches and minor grammar/style edits. All content was reviewed and revised by the authors, and the final manuscript is entirely our own work.

REFERENCES

- [1] C. Choi, W. Schwarting, J. DelPreto, and D. Rus, “Learning object grasping for soft robot hands,” *IEEE Robotics and Automation Letters*, vol. 3, no. 3, pp. 2370–2377, 2018.
- [2] H.-S. Fang, C. Wang, M. Gou, and C. Lu, “Graspnet-1billion: A large-scale benchmark for general object grasping,” in *Proceedings of the IEEE/CVF conference on computer vision and pattern recognition*, pp. 11444–11453, 2020.
- [3] X. Zhang, W. Lv, and L. Zeng, “A 6dof pose estimation dataset and network for multiple parametric shapes in stacked scenarios,” *Machines*, vol. 9, no. 12, p. 321, 2021.
- [4] A. A. Malik, M. V. Andersen, and A. Bilberg, “Advances in machine vision for flexible feeding of assembly parts,” *Procedia Manufacturing*, vol. 38, pp. 1228–1235, 2019.
- [5] S. Peng, Y. Liu, Q. Huang, X. Zhou, and H. Bao, “Pvnet: Pixel-wise voting network for 6dof pose estimation,” in *Proceedings of the IEEE/CVF Conference on Computer Vision and Pattern Recognition*, pp. 4561–4570, 2019.
- [6] S. Zakharov, I. Shugurov, and S. Ilic, “Dpod: 6d pose object detector and refiner,” in *Proceedings of the IEEE/CVF international conference on computer vision*, pp. 1941–1950, 2019.
- [7] Z. Li, G. Wang, and X. Ji, “Cdpm: Coordinates-based disentangled pose network for real-time rgb-based 6-dof object pose estimation,” in *Proceedings of the IEEE/CVF International Conference on Computer Vision*, pp. 7678–7687, 2019.
- [8] J. Cheng, P. Liu, Q. Zhang, H. Ma, F. Wang, and J. Zhang, “Real-time and efficient 6-d pose estimation from a single rgb image,” *IEEE Transactions on Instrumentation and Measurement*, vol. 70, pp. 1–14, 2021.
- [9] G. Wang, F. Manhardt, F. Tombari, and X. Ji, “Gdr-net: Geometry-guided direct regression network for monocular 6d object pose estimation,” in *Proceedings of the IEEE/CVF Conference on Computer Vision and Pattern Recognition*, pp. 16611–16621, 2021.
- [10] G. Zhou, D. Wang, Y. Yan, C. Liu, and Q. Chen, “6-d object pose estimation using multiscale point cloud transformer,” *IEEE Transactions on Instrumentation and Measurement*, vol. 72, pp. 1–11, 2022.
- [11] V. N. Nguyen, T. Groueix, M. Salzmann, and V. Lepetit, “Gigapose: Fast and robust novel object pose estimation via one correspondence,” in *Proceedings of the IEEE/CVF Conference on Computer Vision and Pattern Recognition*, pp. 9903–9913, 2024.
- [12] B. Wen, W. Yang, J. Kautz, and S. Birchfield, “Foundationpose: Unified 6d pose estimation and tracking of novel objects,” in *Proceedings of the IEEE/CVF Conference on Computer Vision and Pattern Recognition*, pp. 17868–17879, 2024.
- [13] J. Lin, L. Liu, D. Lu, and K. Jia, “Sam-6d: Segment anything model meets zero-shot 6d object pose estimation,” in *Proceedings of the IEEE/CVF Conference on Computer Vision and Pattern Recognition*, pp. 27906–27916, 2024.
- [14] T. Höfer, B. Kiefer, M. Messmer, and A. Zell, “Hyperposepdf: hypernetworks predicting the probability distribution on so(3),” in *Proceedings of the IEEE/CVF Winter Conference on Applications of Computer Vision*, pp. 2369–2379, 2023.
- [15] K. Murphy, C. Esteves, V. Jampani, S. Ramalingam, and A. Makadia, “Implicit-pdf: Non-parametric representation of probability distributions on the rotation manifold,” *arXiv preprint arXiv:2106.05965*, 2021.
- [16] J. Sock, G. Garcia-Hernando, and T.-K. Kim, “Active 6d multi-object pose estimation in cluttered scenarios with deep reinforcement learning,” in *2020 IEEE/RSJ International Conference on Intelligent Robots and Systems (IROS)*, pp. 10564–10571, 2020.
- [17] J. Yang, W. Xue, S. Ghavidel, and S. L. Waslander, “Active 6d pose estimation for textureless objects using multi-view rgb frames,” 2025.
- [18] T. Mizuno, K. Yabashi, and T. Tadaki, “Object pose estimation by camera arm control based on the next viewpoint estimation,” in *2024 IEEE/RSJ International Conference on Intelligent Robots and Systems (IROS)*, p. 9482–9487, IEEE, Oct. 2024.
- [19] K. Park, T. Patten, and M. Vincze, “Pix2pose: Pixel-wise coordinate regression of objects for 6d pose estimation,” in *Proceedings of the IEEE/CVF International Conference on Computer Vision*, pp. 7668–7677, 2019.
- [20] Y. He, W. Sun, H. Huang, J. Liu, H. Fan, and J. Sun, “Pvn3d: A deep point-wise 3d keypoints voting network for 6dof pose estimation,” 2020.
- [21] I. Shugurov, S. Zakharov, and S. Ilic, “Dpodv2: Dense correspondence-based 6 dof pose estimation,” *IEEE Transactions on Pattern Analysis and Machine Intelligence*, vol. 44, no. 11, pp. 7417–7435, 2022.
- [22] T. Hodaň, M. Sundermeyer, B. Drost, Y. Labbé, E. Brachmann, F. Michel, C. Rother, and J. Matas, “Bop challenge 2020 on 6d object localization,” in *Computer Vision—ECCV 2020 Workshops: Glasgow, UK, August 23–28, 2020, Proceedings, Part II 16*, pp. 577–594, Springer, 2020.
- [23] R. Shao, W. Li, L. Zhang, R. Zhang, Z. Liu, R. Chen, and L. Nie, “Large vlm-based vision-language-action models for robotic manipulation: A survey,” 2025.
- [24] M. Ahn, A. Brohan, N. Brown, Y. Chebotar, O. Cortes, B. David, C. Finn, C. Fu, K. Gopalakrishnan, K. Hausman, A. Herzog, D. Ho, J. Hsu, J. Ibarz, B. Ichter, A. Irpan, E. Jang, R. J. Ruano, K. Jeffrey, S. Jesmonth, N. J. Joshi, R. Julian, D. Kalashnikov, Y. Kuang, K.-H. Lee, S. Levine, Y. Lu, L. Luu, C. Parada, P. Pastor, J. Quiambao, K. Rao, J. Rettinghouse, D. Reyes, P. Sermanet, N. Sievers, C. Tan, A. Toshev, V. Vanhoucke, F. Xia, T. Xiao, P. Xu, S. Xu, M. Yan, and A. Zeng, “Do as i can, not as i say: Grounding language in robotic affordances,” 2022.
- [25] D. Driess, F. Xia, M. S. M. Sajjadi, C. Lynch, A. Chowdhery, B. Ichter, A. Wahid, J. Tompson, Q. Vuong, T. Yu, W. Huang, Y. Chebotar, P. Sermanet, D. Duckworth, S. Levine, V. Vanhoucke, K. Hausman, M. Toussaint, K. Greff, A. Zeng, I. Mordatch, and P. Florence, “Palme: An embodied multimodal language model,” 2023.
- [26] J. Liang, W. Huang, F. Xia, P. Xu, K. Hausman, B. Ichter, P. Florence, and A. Zeng, “Code as policies: Language model programs for embodied control,” 2023.
- [27] S. Vemprala, R. Bonatti, A. Buckner, and A. Kapoor, “Chatgpt for robotics: Design principles and model abilities,” 2023.
- [28] X. Li, M. Liu, H. Zhang, C. Yu, J. Xu, H. Wu, C. Cheang, Y. Jing, W. Zhang, H. Liu, H. Li, and T. Kong, “Vision-language foundation models as effective robot imitators,” 2024.
- [29] S. Wang, S. Liu, W. Wang, J. Shan, and B. Fang, “Robobert: An end-to-end multimodal robotic manipulation model,” 2025.
- [30] A. Brohan, N. Brown, J. Carbajal, Y. Chebotar, X. Chen, K. Choremanski, T. Ding, D. Driess, A. Dubey, C. Finn, P. Florence, C. Fu, M. G. Arenas, K. Gopalakrishnan, K. Han, K. Hausman, A. Her-

- zog, J. Hsu, B. Ichter, A. Irpan, N. Joshi, R. Julian, D. Kalashnikov, Y. Kuang, I. Leal, L. Lee, T.-W. E. Lee, S. Levine, Y. Lu, H. Michalewski, I. Mordatch, K. Pertsch, K. Rao, K. Reymann, M. Ryoo, G. Salazar, P. Sanketi, P. Sermanet, J. Singh, A. Singh, R. Soricut, H. Tran, V. Vanhoucke, Q. Vuong, A. Wahid, S. Welker, P. Wohlhart, J. Wu, F. Xia, T. Xiao, P. Xu, S. Xu, T. Yu, and B. Zitkovich, “Rt-2: Vision-language-action models transfer web knowledge to robotic control,” 2023.
- [31] M. J. Kim, K. Pertsch, S. Karamcheti, T. Xiao, A. Balakrishna, S. Nair, R. Rafailov, E. Foster, G. Lam, P. Sanketi, Q. Vuong, T. Kollar, B. Burchfiel, R. Tedrake, D. Sadigh, S. Levine, P. Liang, and C. Finn, “Openvla: An open-source vision-language-action model,” 2024.
- [32] R. Wolf, Y. Shi, S. Liu, and R. Rayyes, “Diffusion models for robotic manipulation: A survey,” 2025.
- [33] J. Urain, N. Funk, J. Peters, and G. Chalvatzaki, “Se(3)-diffusionfields: Learning smooth cost functions for joint grasp and motion optimization through diffusion,” 2023.
- [34] H. Ryu, J. Kim, H. An, J. Chang, J. Seo, T. Kim, Y. Kim, C. Hwang, J. Choi, and R. Horowitz, “Diffusion-edfs: Bi-equivariant denoising generative modeling on se(3) for visual robotic manipulation,” 2023.
- [35] R. Freiberg, A. Qualmann, N. A. Vien, and G. Neumann, “Diffusion for multi-embodiment grasping,” 2024.
- [36] B. Lim, J. Kim, J. Kim, Y. Lee, and F. C. Park, “Equigrasflow: SE(3)-equivariant 6-dof grasp pose generative flows,” in *8th Annual Conference on Robot Learning*, 2024.
- [37] T. Zhong and C. Allen-Blanchette, “Gagrasp: Geometric algebra diffusion for dexterous grasping,” 2025.
- [38] N. Funk, J. Urain, J. Carvalho, V. Prasad, G. Chalvatzaki, and J. Peters, “Actionflow: Equivariant, accurate, and efficient policies with spatially symmetric flow matching,” 2024.
- [39] D. Wang, S. Hart, D. Surovik, T. Kelestemur, H. Huang, H. Zhao, M. Yeatman, J. Wang, R. Walters, and R. Platt, “Equivariant diffusion policy,” 2024.
- [40] J. Yang, Z. ang Cao, C. Deng, R. Antonova, S. Song, and J. Bohg, “Equibot: Sim(3)-equivariant diffusion policy for generalizable and data efficient learning,” 2024.
- [41] C. Tie, Y. Chen, R. Wu, B. Dong, Z. Li, C. Gao, and H. Dong, “Et-seed: Efficient trajectory-level se(3) equivariant diffusion policy,” 2025.
- [42] J. Song, C. Meng, and S. Ermon, “Denoising diffusion implicit models,” 2022.
- [43] G. Wang, F. Manhardt, F. Tombari, and X. Ji, “Gdr-net: Geometry-guided direct regression network for monocular 6d object pose estimation,” in *2021 IEEE/CVF Conference on Computer Vision and Pattern Recognition (CVPR)*, pp. 16606–16616, 2021.
- [44] J. Panerati, H. Zheng, S. Zhou, J. Xu, A. Prorok, and A. P. Schoellig, “Learning to fly – a gym environment with pybullet physics for reinforcement learning of multi-agent quadcopter control,” 2021.
- [45] L. Chen, H. Yang, C. Wu, and S. Wu, “Mp6d: An rgb-d dataset for metal parts’ 6d pose estimation,” *IEEE Robotics and Automation Letters*, vol. 7, no. 3, pp. 5912–5919, 2022.
- [46] H. Sun, Y. Wang, Z. Zhou, S. Wang, H. Yang, J. Sun, and Q. Cao, “Exploring pose-guided imitation learning for robotic precise insertion,” 2025.